Helical Undulator Design for Inverse Free Electron Laser Interaction

Alex Strelnikov
University of Rochester, Class of 2010
Faculty Advisor: Professor Musumeci
UCLA Physics REU, Summer 2009

Abstract. This paper will deal with the preliminary optimization of a helical undulator design for an inverse free electron laser experiment set to take place at Brookhaven National Laboratory in 2010. The paper will first describe the IFEL interaction and discuss its advantages. IFEL theory will then be presented for helical geometry with a comparison between this and the planar case. The paper will then describe the choices made in order to optimize acceleration in simulations.

1. Introduction

The acceleration and manipulation of high energy particle beams has become an integral part of modern physics. The conventional method of doing so, however, comes with a scale and cost that has just about gotten out of hand with costs in the billions of dollars and lengths reaching tens of kilometers. Alternative methods of acceleration have thus become a highly attractive area of research. The inverse free electron laser scheme is one such alternative. It uses very high energy radiation to accelerate charged particles in a very short distance.

It works by having a beam of relativistic electrons sent through an undulator. This is an array of magnets arranged to create an oscillating field that gives the beam a small transverse velocity. An electromagnetic wave is also sent through the undulator parallel to the direction of the beam's travel. As the electrons oscillate down the length of the undulator, they gain energy from the laser beam. The experiment taking place in 2010 at BNL hopes to achieve an energy gain of more than 170 MeV from an initial energy of 50 MeV. This acceleration will take place in a distance of only 60 cm giving rise to an energy gradient of over 200 MeV/m. This energy gradient is an order of magnitude larger than what is being achieved in conventional accelerators.

However, this accelerator scheme is not a feasible option for future high energy colliders as the transverse oscillation creates synchrotron radiation that would become too great compared with the energy gain at energies greater than 10 GeV. The main applications of IFEL acceleration center around medium energy electrons being used to create a good source of x-rays either through ICS or FEL.

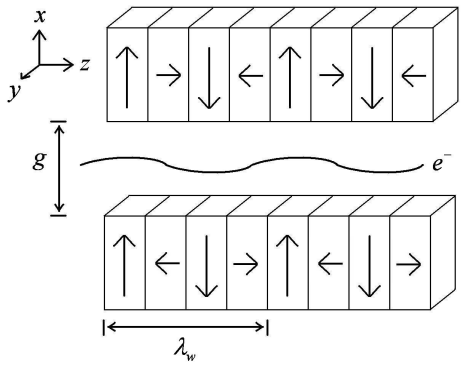

FIGURE 1

To date, IFEL experiments have been done using planar geometry, meaning that the beam oscillates only in one dimension. Figure 1 shows the planar case, with the electron's path through the undulator. There are four permanent magnets per undulator period, λ_w, with arrows showing the direction of magnetization. For a large enough gap size, g, the on axis field created by this undulator is $\mathbf{B}(z) = (B_0 cos(k_w z), 0, 0)$, where k_w is the undulator wave number.

The experiment taking place next year will be the first to use helical geometry. The undulator will produce oscillating fields in two dimensions that will cause the electrons to take a helical path. This arrangement turns out to be advantageous, but due to technical difficulties associated with building a helical undulator, the geometry has for the most part been passed over. This paper will discuss these difficulties and the process of optimizing the design for the helical undulator to be used next year.

2. Helical IFEL Theory

2.1. **Accelerator Equations.** Contrary to the planar case, where the magnetic field oscillates in only one dimension, the helical case magnetic field oscillates in both x and y as shown in equation (1).

$$\mathbf{B}(z) = B_0 \left(cos\left(k_w z\right), sin\left(k_w z\right), 0\right) \tag{1}$$

One of the consequences of this magnetic field is that the helical interaction takes advantage of circularly polarized light as opposed just a plane wave. When the fields of the undulator and laser are combined, the Lorentz force law for the system then becomes:

$$m\frac{d\gamma \mathbf{v}}{dt} = e\mathbf{E_l} + e\beta \times (\mathbf{B_l} + \mathbf{B_w}) \tag{2}$$

Another observation is that the transverse momentum is conserved since ideally both the laser and undulator fields depend only on z.

$$\mathbf{p}_\mathrm{T} = m\gamma \mathbf{v_T} + e\left(\mathbf{A_l} + \mathbf{A_w}\right) \tag{3}$$

Next, the Lorentz force law in (2) can be rewritten to give the energy gain as a function of time in the form of:

$$mc^2\frac{d\gamma}{dt} = e\mathbf{v_T} \cdot \mathbf{E_l} \tag{4}$$

(3) and (4) can now be combined to derive the accelerator equations. First, it is good to define several terms that make the written out equations more concise. $K = eB_w/mck_w$ and $K_l = eE_l/mc^2k$ are the undulator and laser parameters respectively. $\psi = k_w z + kz - \omega t$ is a phase relation between the motion of the electrons and the electromagnetic field oscillation of the laser. The accelerator equations become:

$$\frac{d\gamma}{dz} = kK\frac{K_l}{\gamma}sin\psi \tag{5}$$

$$\frac{d\psi}{dz} = k_w - k\frac{1 + K^2 + K_l^2}{2\gamma^2} \tag{6}$$

When this problem is solved for planar geometry, the only difference in equation (5) is a Bessel function term, JJ/2, in the numerator on the right hand side of the equation. Equation (6) also contains a factor of JJ/2 in the numerator of the fraction on the ride hand side. The JJ term is never greater than .8, meaning that the helical IFEL interaction creates more than twice the energy gain per unit length than the planar case. This can also be seen through equation (4), which shows that the energy gain is directly proportional to the magnitude of the transverse velocity. In the planar case, this velocity is zero at two different points along each period of transverse oscillation. In the helical case, however, the amplitude of the transverse velocity is constant and nonzero.

2.2. **Resonant Condition.** Another important aspect of equation (4) to analyze is the dot product between the transverse velocity and the electric field of the laser. Both of these vectors oscillate in sign throughout the length of the pendulum. Therefore, if the undulator period is simply chosen at random creating electron oscillations that are not tailored to the field of the laser, $d\gamma/dt$ will also oscillate in sign. Over time, this will create a net zero energy gain.

In order to keep $d\gamma/dt$ positive, it becomes necessary to keep the electrons in the same relative phase as the electric field of the laser. In other words, $d\psi/dz$ must be equal to zero throughout the undulator. Equation (6) then simplifies to the following relation known as the resonant condition.

$$\lambda = \frac{\lambda_w\left(1 + K^2\right)}{2\gamma^2} \tag{7}$$

Because the wavelength of the laser is constant and the goal is to increase the energy of the electrons, the resonant condition leads to the tapering of the undulator. As γ increases down the length of the undulator, λ_w must increase as well. Using the relation in (7), (5) can be solved to create a differential equation for how λ_w must change down the length of the undulator to maximize the energy gain.

3. Energy Gain Optimization

3.1. **Optimization of Laser Parameters.** The laser being used for this experiment is the .5 TW 10.6 μm laser located at BNL. Although the wavelength and power of the laser are predetermined, the focusing can be tailored for the experiment in order to optimize the acceleration.

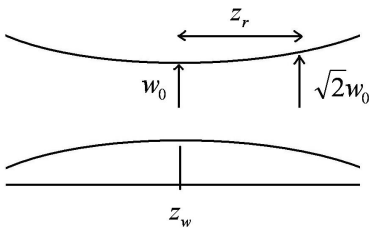

FIGURE 2

Figure 2 is a diagram of how the laser beam size changes as a function of distance. The Rayleigh range, denoted by z_r, is defined as the distance over which the cross sectional area of the beam doubles. The smallest radius of the beam is called the waist, w_0, the location of which is denoted by z_w. The optimal focusing for the interaction places the waist at halfway down the length of the undulator.

The optimal Rayleigh range also lies in a middle ground between a very small and large length. If the Rayleigh range is too small, the laser will be very intense around the waist. However, this intensity will drop off very quickly, and will be too small throughout the majority of the undulator for effective energy gain to take place. At the other extreme, if the the Rayleigh range is very large, the intensity will be too great in many parts of the undulator. Some middle ground should maximize the energy gain, and this is evidenced by simulation.

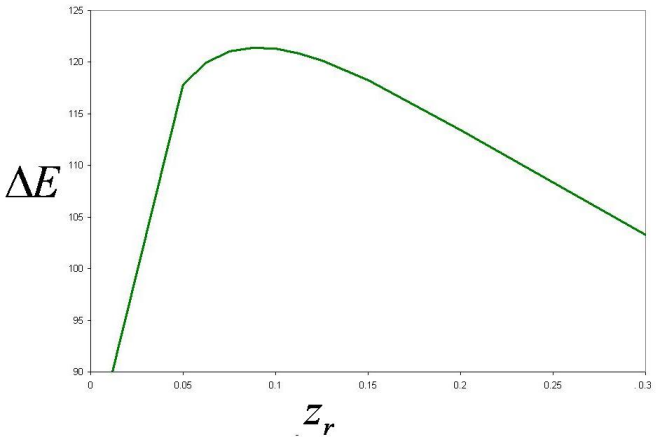

FIGURE 3

Figure 3 shows a graph of data obtained from a one dimensional simulation of the resonant condition showing that a Rayleigh range of 8.75 cm maximizes the energy gain.

3.2. **Undulator Array Optimization.** Another choice to be made is the type of array used to create the undulator. The first option is to use the Halbach array. This is the array shown in figure 1 depicting the planar IFEL interaction. To create a helical field out of this arrangement, one would simply add a third and fourth Halbach array to either side of the axis offset by half of an undulator wavelength. The advantage of using this arrangement is that it has been widely studied and used for both the FEL and the planar

IFEL interactions. However, since it is an array specifically designed to create an oscillating field along one dimension, it is not necessarily the best choice when considering helical geometry.

The other choice, which is used in all of the simulations presented in this paper, is depicted in figure 4.

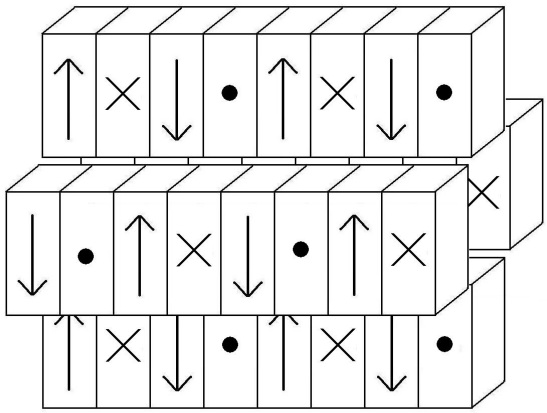

FIGURE 4

For sufficient distances away from the magnets, this array creates the same helical field as the undulator made with Halbach arrays. From this point in the paper, this array type will be referred as the coupled helical array, because unlike in the case with Halbach arrays, this type of undulator cannot be separated into pairs of arrays that each create a field that oscillates in one dimension.

The advantage of the Halbach array becomes the disadvantage of the coupled helical array as it has not been widely studied or used. Therefore, it is not yet confirmed to be as or more effective than the Halbach array would be for the helical interaction. The advantages of the coupled helical array are that for the same magnet dimensions, it obtains a 6 percent higher magnetic field amplitude than the Halbach array, and it also maintains the ideal sinusoidal field for smaller undulator gap sizes. The second advantage is particularly important, because the IFEL theory was derived assuming a perfectly sinusoidal undulator field, and deviations from this would likely cause less energy gain.

The difference between the two array types in this regard can be summarized by the magnetic field amplitude as a function of the ratio of the distance away from the magnets to the undulator wavelength. For the Halbach array, the magnetic field ideally drops off as $B \propto e^{-k_w y}$, where y is the distance away from the magnets. Plugging in $g/2$ for y gives the ideal amplitude along the axis of the undulator as $B \propto e^{-\pi g/\lambda_w}$. However, this condition only holds for relatively large ratios of gap to undulator period as shown in figure 5.

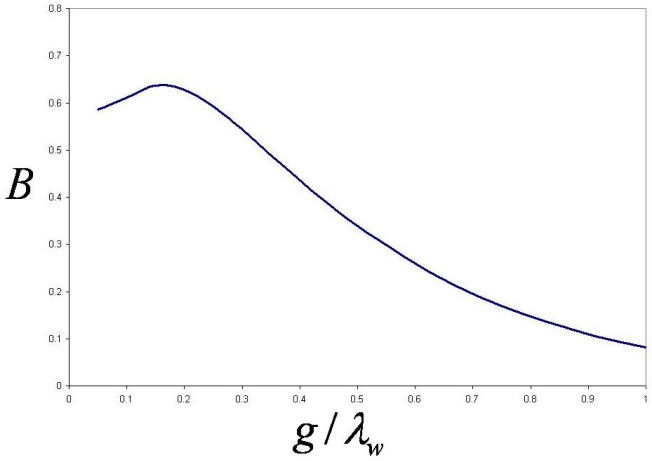

FIGURE 5

This graph shows the magnetic field amplitude for the Halbach array. The exponential condition begins to fail at a ratio of about .25. In comparison, figure 6 shows the same relation for the coupled helical array, for which the exponential relation does not fail until a ratio of about .15. Incidentally, the ratio at which the exponential relation fails is also the ratio at which the fields start to considerably deviate from sinusoidal.

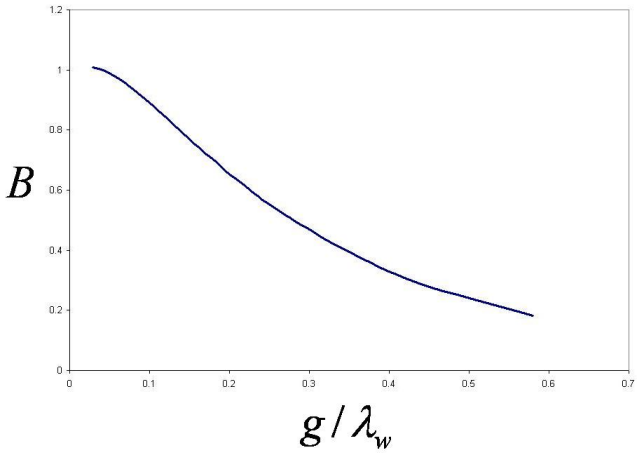

FIGURE 6

In order to keep the field close to the ideal sinusoidal field, the ratio of the gap to undulator wavelength was kept to within the range in which the exponential relation holds. This way, the magnetic field amplitude could be accounted for by an analytic function as it is increased by the undulator tapering.

3.3. **Optimized Undulator Field.** Now that the laser focusing is optimized and there is a relation between the magnetic field amplitude and the ratio g/λ_w, the differential equation for the optimized undulator period becomes:

$$\frac{d\lambda_w}{dz} = \frac{8\pi sin\psi K K_l}{1 + K^2\left(3 + k_w g\right)}\left[1 + \left(\frac{z - z_w}{z_r}\right)^2\right]^{-1/2} \tag{8}$$

This equation can be numerically solved with the optimized parameters to get the the ideal undulator period.

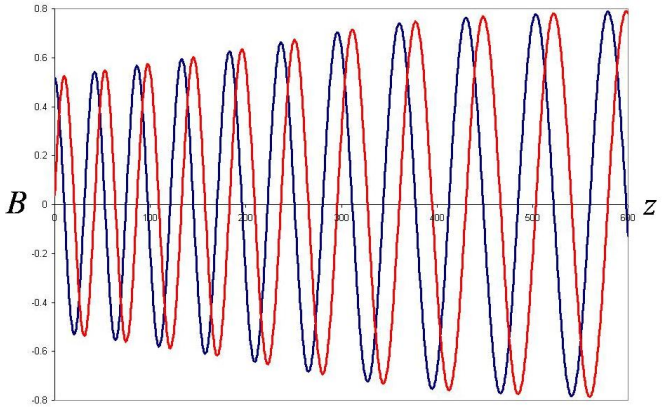

FIGURE 7

This field is then used with the particle tracker code TREDI to simulate the helical interaction, and determine the energy gain. Figure 8 shows the maximum energy of the simulated electrons down the length of the undulator.

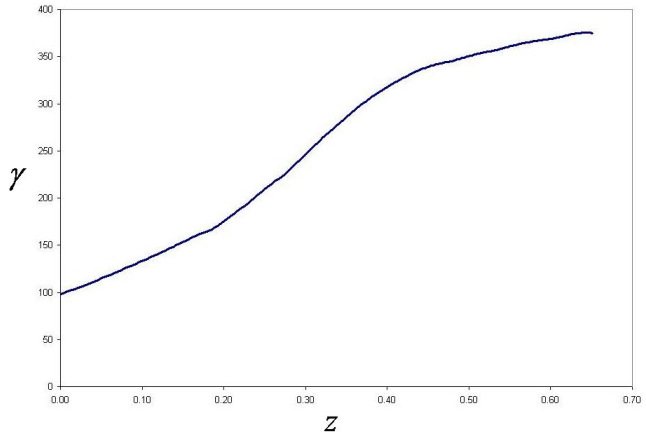

FIGURE 8

This graph represents an energy gain of 141.5 MeV, translating to an energy gradient of 235.8 MeV/m for the undulator.

4. Recreating the Ideal Field

The remaining challenge is to recreate this ideal field with as much accuracy as possible. When considering the cost, it is best to update the period of the undulator to match the period as little as possible. This way, many more of the magnets to be ordered have the same dimensions. On the other hand, in order to get the best possible fit to the ideal field, it is best to update the period as many times per period as there are magnets. It turns out that with the strong tapering, the period cannot be updated at integer multiples of a wavelength. This is because the undulator period is always increasing down the length of the undulator. Every time the period increases, so does the magnitude of the field. This increase in field must occur at alternating signs of the field, or else the particle beam can never fly straight. Therefore, in order to get a good fit, and keep the undulator from being as expensive as possible, the period is updated every half wavelength or two magnets.

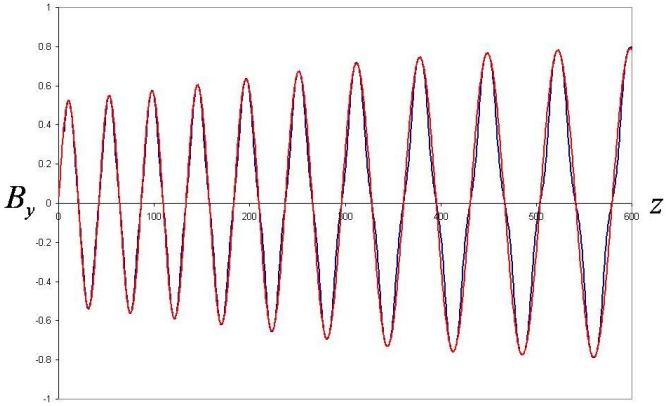

FIGURE 9

Figure 9 shows a comparison of the ideal field to that of the calculated undulator. Upon closer inspection, one can see the deviation from the ideal sinusoidal shape, especially in the last third of the undulator where the ratio g/λ_w is smallest.

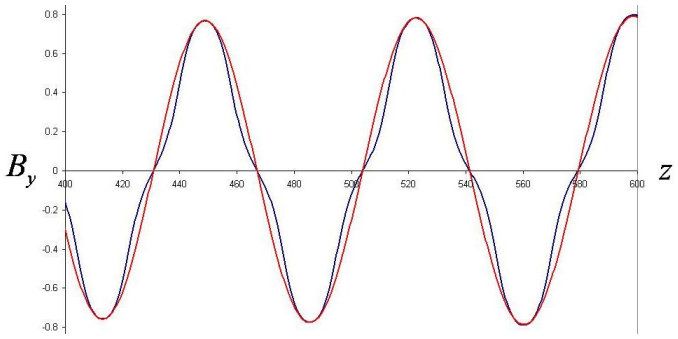

FIGURE 10

To see what effect the deviation had on the acceleration, this field was used with the TREDI simulation. The resulting energy gain was 125.9 MeV, making the energy gradient 209.8 MeV/m. This is a loss of 11 percent created by the deviation from the ideal field, which is a fairly considerable loss. However, this simulation still shows an energy gradient of over 200 MeV/m, which would make the experiment a success.

5. Work Left to be Done

Although the data presented in this paper gives good reason to believe that the helical IFEL experiment will be successful, there is still much more that can be done to better model the interaction.

5.1. **1D vs 3D.** All of the data presented in this paper came from simplified models. The Mathcad simulations were done by an entirely one dimensional solution of a differential equation. The TREDI data was achieved through a three dimensional simulation. However, the three dimensional nature of the magnetic field was ignored. This simplification comes at the cost of accurately predicting the behavior of the electrons. Since the electrons have a transverse oscillation, they do not stay on the axis of the undulator. Off of this axis, the magnetic field differs, which would change the interaction. Therefore, a full three dimensional simulation is important to judge the probability of success for this experiment.

5.2. **Further Study of Undulator Field.** The real undulator magnetic field is far from the simple sine curve that is derived with the assumption that the undulator wavelength is considerably smaller than the gap. A better study of this field could give a more precise theoretical understanding of the IFEL interaction. One possible way to approach the problem is considering that very close to the magnets, the field is a step function that can be taken as a sum of Fourier series:

$$B = B_0 \sum_{n=1}^{\infty} \frac{2\sqrt{2}}{(2n-1)\,\pi} sin\left[(2n-1)\,k_w z + \frac{\pi}{4}\,(-1)^n\right] \tag{9}$$

Then a more accurate model of the field, taking the deviation into account could be:

$$B = B_0 \sum_{n=1}^{\infty} e^{-(2n-1)k_w y} \frac{2\sqrt{2}}{(2n-1)\,\pi} sin\left[(2n-1)\,k_w z + \frac{\pi}{4}\,(-1)^n\right] \tag{10}$$

So that for large $k_w y$, $B \propto e^{-k_w y} sin\,(k_w z + \delta)$.

5.3. **More Study of the Array Choices.** As stated previously, the Halbach array comes with a distinctive advantage of being well known. It is therefore necessary to study the differences between it and the coupled helical array to find out which is the best solution for helical geometry.

6. Conclusions

As the data presented in this paper suggests, the coupled helical array should be successful in providing an energy gradient of more than 200 MeV/m for next year's experiment. However, more precise modeling is needed for a more definitive answer. It is also too early to make a concrete decision as to which array type would work best for the experiment.

7. Acknowledgements

I would like to thank Professor Pietro Musumeci for his time and help during the summer. I would also like to thank Francoise Queval for organizing the program and the NSF for funding my experience.

8. References

Clarke, James A. *The Science and Technology of Undulators and Wigglers.* New York: Oxford UP, 2004. Print.

Musumeci, Pietro. "Acceleration of Electrons by Inverse Free Electron Laser Interaction." Diss. University of California Los Angeles, 2004. Print.

Reiche, Sven. "Numerical Studies for a Single Pass High Gain Free Electron Laser." Diss. University of Hamburg, 1999. Print.